J Polym Res (2016) 23: 223
DOI 10.1007/s10965-016-1115-1

ORIGINAL PAPER

Preparation of thermo-responsive electrospun nanofibers containing rhodamine-based fluorescent sensor for Cu^{2+} detection

Wen-Chung Wu [1] · **Hsiao-Jen Lai** [1]

Received: 7 June 2016 / Accepted: 28 September 2016 / Published online: 6 October 2016

Abstract A series of Cu^{2+}-sensing nanofibers has been successfully prepared by electrospinning of poly[(N-isopropylacrylamide)-*co*-(*N*-hydroxymethyl acrylamide)-*co*-(4-rhodamine hydrazonomethyl-3-hydroxy-phenyl methacrylate)] [poly(NIPAAm-*co*-NMA-*co*-RHPMA), PNNR] random copolymers. These PNNR copolymers were synthesized by free radical copolymerization of three monomers, thermo-responsive NIPAAm, chemically crosslinkable NMA and Cu^{2+}-sensing RHPMA, with the composition of RHPMA in the range of 2.4–16.3 wt%. In acidic environments, the PNNR copolymers showed highly selective and sensitive recognition and displayed "ON-OFF" fluorescence toward Cu^{2+} both in solution and in solid state (thin films and nanofibers). From the quantitative analysis via Stern-Volmer plots, PNNR nanofibers exhibited comparable Stern-Volmer constants as those of PNNR solutions in the order of 10^4 M^{-1}, which are much higher than those of PNNR thin films. The enhanced sensitivity of PNNR electrospun nanofibers is attributed to their higher surface area compared to dip-coating films. The PNNR nanofibers also exhibited an on/off switchable sensing behavior in response to temperature change due to the hydrophilic-hydrophobic transition of PNIPAAm. In addition, the binding of PNNR with Cu^{2+} is chemically reversible both in solution and in nanofibers with the treatment of Na_4EDTA.

Keywords Electrospinning · Nanofiber · Sensor · Rhodamine · Thermo-responsive materials

Introduction

Recently, the development of sensors with high selectivity and sensitivity for the detection of trace metal ions either as biologically essential elements or as environmentally hazardous pollutants has gained a considerable interest [1–4]. Currently, various types of metal-ion sensors, such as chemosensors, optical sensors, and electrochemical sensors, have been explored to pursuit better performance and more economical devices [5–7]. Among them, optical sensors based on colorimetric and/or fluorescent mechanisms are of great interests due to their high sensitivity, selectivity, quick response and potential for localized detection [8]. Even though a wide variety of materials, including organic molecules [8, 9], conjugated polymers [10, 11], and quantum dots [12, 13], has been developed and demonstrated as optical metal-ion sensors with superior selectivity and sensitivity, most of them were studied in either organic or aqueous solution, which is difficult to separate and recycle the sensors. The development of sensors based on thin films or membranes may overcome these drawbacks, but their practical application is usually prohibited by their low sensitivity due to low solid–liquid interfacial area [14]. Thus, electrospun nanofibers with a high specific surface area have emerged as a new material platform for novel sensing devices [15].

Among various metal ions, copper ion (Cu^{2+}) is an essential trace element in biological system, and the disorder in uptake, storage, and trafficking of copper ions might be

Electronic supplementary material The online version of this article (doi:10.1007/s10965-016-1115-1) contains supplementary material, which is available to authorized users.

✉ Wen-Chung Wu
wcwu@mail.ncku.edu.tw

[1] Department of Chemical Engineering, National Cheng Kung University, Tainan 70101, Taiwan

associated with some severe diseases, such as Alzheimer's and Wilson's diseases [16–19]. Thus, quantitative detection of trace concentration and tracking biological distribution of copper ions would be of significant importance. Up to date, a great amount of colorimetric and/or fluorescent sensors have been prepared and evaluated for Cu^{2+} detection [20–23]. Representative mechanisms for copper ion recognition are Cu^{2+}-induced spirolactam ring-opening process [24], hydrolysis process [25], oxidation process [26], and oxidative cyclization process [27]. Among different types of optical metal-ion sensors, the rhodamine-based derivatives have been recognized as an ideal platform for constructing colorimetric and fluorescent sensors due to their extraordinary photophysical properties [28]. The cation-sensing mechanism of rhodamine-based probes is attributed to the spirolactam ring-opening process triggered by cation binding [8]. The originally colorless and nonfluorescent rhodamine moieties with spirolactam structure would transit into pink in color with orange fluorescence resulting from the formation of ring-opening amide due to proton or metal-ion binding. Nevertheless, most rhodamine-based probes exhibited the "OFF-ON" sensing characteristic, only few examples showed the "ON-OFF" optical response toward cation binding [22, 23].

In this study, we report the preparation of new Cu^{2+}-sensing electrospun (ES) nanofibers based on random copolymers, poly[(N-isopropylacrylamide)-*co*-(*N*-hydroxymethyl acrylamide)-*co*-(4-rhodamine hydrazonomethyl-3-hydroxy-phenyl methacrylate)] [poly(NIPAAm-*co*-NMA-*co*-RHPMA), PNNR], synthesized by free radical polymerization. The multifunctional copolymers are composed of different compositions of thermo-responsive NIPAAm, chemically cross-linkable NMA, and Cu^{2+}-responsive RHPMA moieties. The NMA moiety plays an important role to maintain the ES nanofibers intact in water by the chemical cross-linking after thermal treatment. The RHPMA moiety acts as fluorescent sensing units and exhibits changes in fluorescent characteristics after chelation with copper ions. The chemical structures of all polymers were identified by ^{1}H-NMR and size exclusion chromatography (SEC). Through delicate control of copolymer compositions and an appropriate cross-linking protocol, the corresponding nanofibers with stable morphologies in aqueous solution were prepared by the electrospinning technique with a single-capillary spinneret. The morphology of ES nanofibers was investigated by field-emission scanning electron microscope (FE-SEM). The performances for optical sensing and thermo-responsive properties were explored by UV-visible and photoluminescence spectrometry. Herein, we systematically investigated the correlation between the Cu^{2+} sensing characteristics with the states of copolymers (solution, nanofiber and dip-coated film). In addition, we also demonstrated a thermo-responsive on-off switchable sensitivity toward Cu^{2+} ions and a reversibility test via EDTA regeneration.

Material and methods

Materials

N-Isopropylacrylamide (NIPAAm, Adrich) and azobisisobutyronitrile (AIBN, Aldrich) were recrystallized from hexane prior to use. *N*-hydroxymethylacrylamide (NMA, Aldrich), Rhodamine B, hydrazine hydrate, 2,4-dihydroxybenzaldehyde, methacryloyl chloride, trimethylamine, and benzyltriethylammonium chloride (BTEAC, Aldrich) were used as received. Rhodamine B hydrazide and rhodamine hydrazone were synthesized as the reported procedures [29, 30]. Common organic solvents for synthesis were obtained commercially and used as received unless otherwise noted. For metal ion test, solutions of metal ion salts of zinc acetate, potassium acetate, calcium chloride, magnesium chloride, copper chloride, iron chloride, cadmium chloride, and lead acetate were purchased from Aldrich. The mercury ion solution was purchased from J. T. Baker.

Synthesis of 4-rhodamine hydrazonomethyl-3-hydroxy-phenyl methacrylate (RHPMA)

Rhodamine hydrazone (**1**, 2.0 g, 3.48 mmol) and trimethylamine (1.0 ml, 7.18 mmol) were dissolved in 100 ml dry dichloromethane. Then, the solution of methacryloyl chloride (0.37 ml, 7.18 mmol) in dry dichloromethane (1.0 ml) was dropped slowly with stirring at ice bath. Then the reaction solution was allowed to stir at room temperature under N_2 atmosphere overnight. After that, the reaction solution was poured into DI water (50 ml) and extracted with dichloromethane (100 ml). The organic layer was dried over anhydrous $MgSO_4$, filtered and concentrated. The crude product was purified with column chromatography. RHPMA was obtained as yellow powder (1.1 g, yield: 49 %) ^{1}H NMR(400 MHz, $CDCl_3$), δ(ppm): 1.16(t, 12H), 2.02(s, 3H), 3.33(q, 8H), 5.72(s, 1H), 6.27(dd, 2H), 6.29(s, 1H), 6.46(d, 2H), 6.49(d, 2H), 6.57(dd, 1H), 6.62(d, 1H), 7.09(d, 1H), 7.18(d, 1H), 7.52(m, 2H), 7.98(d, 1H), 9.17(s, 1H), 11.05(s, 1H). Elemental analysis, cald. for $C_{39}H_{40}N_4O_5$, C 72.65, H 6.25, N 8.69 %; found, C 72.21, H 6.30, N 8.75 %.

Synthesis of poly[(N-isopropylacrylamide)-*co*-(*N*-hydroxymethyl acrylamide)-*co*-(4-rhodamine hydrazonomethyl-3-hydroxy-phenyl methacrylate)] [poly(NIPAAm-*co*-NMA-*co*-RHPMA) random copolymers, (PNNR1-PNNR3)]

Poly(NIPAAm-*co*-NMA-*co*-RHPMA) was synthesized under the conditions of different molar ratios of NIPAAm, NMA and RHPMA monomers (Table 1) in a 25-ml Schlenk Tube with a magnetic stir bar with AIBN as initiator. NIPAAm (1 g,

Table 1 Composition and properties of poly(NIPAAm-*co*-NMA-*co*-RHPMA)

Polymer	Feed molar ratio NIPAAm:NMA:RHPMA	Copolymer composition[a] x:y:z	M_n[b] [kDa]	PDI[b]	LCST[c] [°C]
PNNR1	300:150:20	1:0.51:0.05	85.3	1.78	61.2
PNNR2	300:150:10	1:0.48:0.02	90.1	1.72	59.4
PNNR3	300:150:5	1:0.52:0.009	92.3	1.65	58.2

[a] Molar ratios estimated from ^{1}H NMR spectra; [b] Determined by SEC using the DMF eluent; [c] LCSTs were determined by observing the 50 % optical transmittance of copolymer solutions at 600 nm using a UV–vis. spectrometer

8.8 mmol), NMA (447 mg, 4.4 mmol), RHPMA (380 mg, 0.59 mmol for PNNR1, 190 mg, 0.29 mmol for PNNR2, and 48 mg, 0.15 mmol for PNNR3) and AIBN (6 mg, 0.04 mmol) were added to Schlenk Tube and dissolved in 10 mL MeOH/toluene (*v/v*, 1:1) mixture. Nitrogen was bubbled through the mixture for 20 min and then, degassed by three freeze-pump-thaw cycles. The reaction mixture was stirred under positive nitrogen pressure and placed into an oil bath at 65 °C overnight. After polymerization, the resulting reaction solution was dialyzed against ultrapure water with a dialysis membrane (molecular weight cutoff of 3500 g mol^{-1}) for 3 days. Then, the copolymers were precipitated in anhydrous diethyl ether and dried in vacuum oven at 40 °C to afford white powders (PNNR1: 1.40 g, 77 %; PNNR2: 1.31 g, 80 %; PNNR3: 1.35 g, 84 %). ^{1}H NMR (400 MHz, *d*-DMSO) δ 0.8–1.2 [−(C***H***$_3$)$_2$], 1.2–2.2 (backbone), 3.8–4.0 [−C***H***-(CH$_3$)$_2$], 4.4–4.7 [−C***H***$_2$-OH], 5.3–5.6 (−O***H***), 6.3–6.5 (aromatic proton), 6.6–6.7 (aromatic proton), 7.1–7.2 [−N***H***-CH-(CH$_3$)$_2$], 8.0–8.1 (−N***H***-CH$_2$-OH), 9.0–9.1 (−N-N = C***H***-), 10.6–10.8 (C$_6$H$_2$-O***H***).

Preparation of electrospun nanofibers and dip-coating films

Poly(NIPAAm-*co*-NMA-*co*-RHPMA) copolymers (PNNR1-PNNR3) were dissolved in methanol with polymer concentration of 20 wt%. In order to enhance the conductivity of electrospun solution, 5 wt% benzyl triethyl-ammonium chloride (BTEAC, corresponding to copolymer) was added and the mixture was stirred for 1 day before fabricating the ES fibers. The ES nanofibers were prepared using a single-capillary spinneret. First, the polymer solution was fed into the syringe pump (Chemyx Fusion 100, USA) connected to the 22 gauge metallic needle, with feed rate of 0.1 mL hr^{-1}. The metallic needle was connected to a high voltage power supply (You-Shang Technical Corp., Taiwan), and a piece of aluminum foil or glass was placed 15 cm below the tip of the needle to collect the ES fibers, and the spinning voltage was set at 10.0 kV. All experiments were carried out at room temperature and around 60 % relative humidity. For the comparison with the properties of the ES nanofibers, the corresponding polymer films were prepared on glass substrate with the same concentration of copolymer by dip-coating method and dried in an airflow hood. The above ES nanofibers or films were thermally cured at 110 °C for 72 h in the dried oven to carry out chemical crosslinking between NMA moieties.

Characterization

^{1}H NMR spectra were measured in $CDCl_3$ and DMSO-d6 by using a Bruker-DPX-400 instrument spectrometer. The molecular weights and polydispersity of PNNR1-PNNR3 copolymers were analyzed by size exclusion chromatography (SEC) with a Waters 1515 pump and a Waters 2410 refractive index (RI) detector, in reference with a series of PS standards and DMF as the eluent. The morphologies of the ES nanofibers were characterized by field-emission scanning electron microscopy (FE-SEM, Hitachi S-4800). The images were taken using a microscope operated at an accelerating voltage of 15 kV. Before imaging, the samples were sputtered with Pt. The average diameter of nanofibers was estimated over 50 fibers in SEM images from each sample. The absorption spectra were measured with a Shimadzu UV-2450 spectrophotometer. The photoluminescence spectra (PL) were recorded on a Hitachi F-4500 spectrophotometer at excitation wavelength of 520 nm. The ES nanofibers or dip-coating films were fixed on the quartz by adhesive tape and put diagonally in the cuvettes filled with Cu^{2+} solution at the concentration of 10^{-6} to 10^{-4} M. All samples were equilibrated for 5 min at each metal ion concentration before PL measurement.

Results and discussion

Synthesis and characterization of RHPMA and poly(NIPAAm-*co*-NMA-*co*-RHPMA) copolymers

The Cu^{2+}-sensing monomer, RHPMA, is composed of Cu^{2+}-chelating rhodamine hydrazone and methacrylate moieties for free radical polymerization. As shown in Scheme 1, RHPMA was prepared by the condensation reaction between methacryloyl chloride and rhodamine hydrazone. The ^{1}H-NMR spectrum (Fig. S1) and elemental analysis have shown the successful synthesis of RHPMA. Poly(*N*-

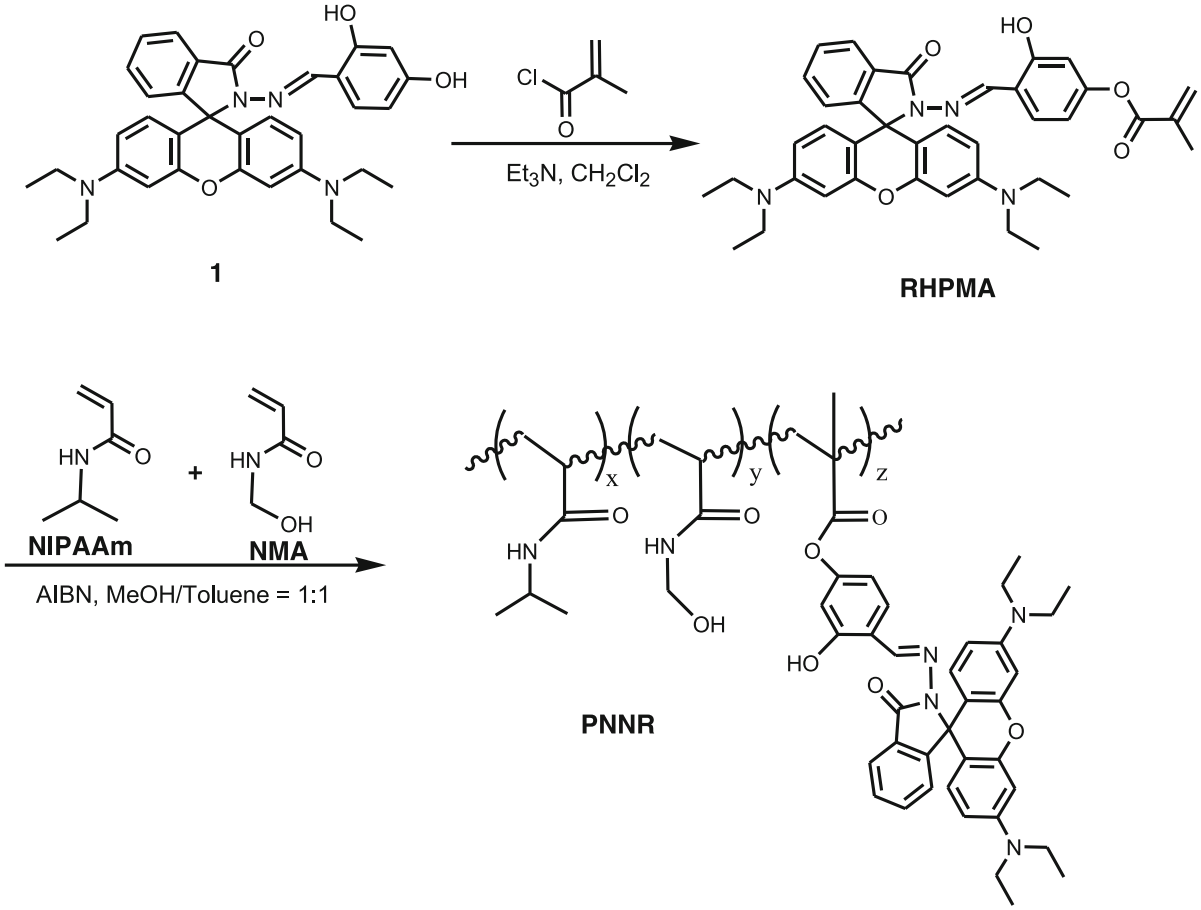

Scheme 1 Synthetic scheme of RHPMA and poly(NIPAAm-*co*-NMA-*co*-RHPMA) (PNNR)

isopropylacrylamide)-*co*-poly(*N*-methylolacrylamide)-*co*-poly(RHPMA) [Poly(NIPAAm-*co*-NMA-*co*-RHPMA), PNNR1-PNNR3] copolymers with different RHPMA monomer compositions were prepared by free radical polymerization (Scheme 1). After purification, PNNR1-PNNR3 copolymers were fully characterized using size exclusion chromatography (SEC) and ^{1}H-NMR. As shown in Fig. S2, the characteristic resonances of NIPAAm, NMA and RHPMA were observed in ^{1}H-NMR spectra and the chemical compositions of the copolymers were determined by comparing the -C**H**$_2$-NH- proton signal at approximately 3.83 ppm of NIPAAm, the -C**H**$_2$-NH- protons at 4.51 ppm from NMA moiety, and the aromatic protons at 6.3–6.5 ppm from RHPMA moiety. The corresponding chemical and physical properties of the prepared copolymers are summarized in Table 1, and the copolymer composition (x:y:z) for PNNR1-PNNR3 determined by NMR peak intensity were similar to the feeding composition. The weight ratios are 2.4, 7.1, and 16.3 % for PNNR1, PNNR2, and PNNR3, respectively. The number-average molecular weights (M_n) of the PNNR1-PNNR3 copolymers evaluated by SEC are 85.3, 90.1, and 92.3 kDa, with the corresponding PDI of 1.78, 1.72, and 1.65, respectively. The slightly lower molecular weight and broader distribution for copolymers with higher RHPMA content could be attributed to the copolymerization of more bulky RHPMA monomers. The thermo-responsive behaviors of PNNR copolymers in

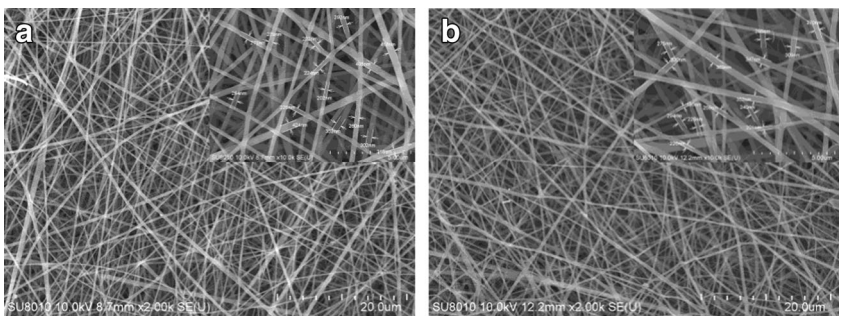

Fig. 1 FE-SEM images of as-spun ES nanofibers of PNNR2 (**a**) and PNNR3 (**b**), the insets show the corresponding size distributions of fibers

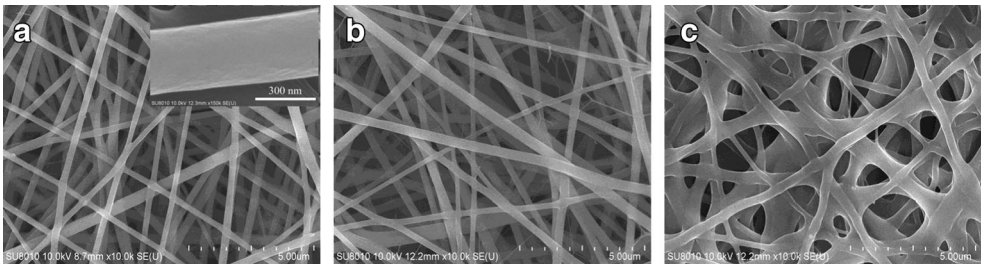

Fig. 2 FE-SEM images of the PNNR2 nanofibers: (**a**) as-spun, (**b**) thermally cross-linked, and (**c**) immersed in DI water at room temperature. The inset in (**a**) shows the enlarged FE-SEM image of the nanofibers

aqueous solution were evaluated by temperature-controlled UV-visible spectroscopy. The lower critical solution temperatures (LCSTs) were determined by observing the 50 % optical transmittance of polymer solution at 600 nm as a function of temperature (Fig. S3). The LCSTs has been shown to increase compared to the reported PNIPAAm homopolymer (32 °C) due to incorporation of the hydrophilic NMA and RhBMA moiety into copolymers [31, 32]. Higher RHPMA content therefore correlates with higher LCST.

Morphologies of poly(NIPAAm-*co*-NMA-*co*-RHPMA) electrospun nanofibers

The poly(NIPAAm-*co*-NMA-*co*-RHPMA) nanofibers were fabricated by electrospinning of a 20 wt% polymer solution with adding 5 wt% BTEAC salt to increase the conductivity of the polymer solution in methanol. With the assistance of BTEAC salt, a continuous fiber mat could be fabricated without bead formation [33]. However, PNNR1 nanofiber was not successfully prepared by electrospinning technique under various process parameters. This might be owing to the highest RHPMA content of PNNR1 copolymers inhibits chain entanglement during the electrospinning process. Figure 1 shows the FE-SEM images of PNNR2 and PNNR3 electrospun (ES) nanofibers in a dry state, and the corresponding average diameters were estimated based on calculating a statistical average of 50 fibers from each image. The average diameters of as-spun PNNR2 and PNNR3 nanofibers are 298 ± 70 and 268 ± 23 nm, respectively. The range of fiber diameter was slightly enlarged with increasing RHPMA composition, which is probably resulted from the higher content of rigid rhodamine moieties. Nevertheless, the as-spun nanofibers with high hydrophilicity at room temperature could not be able to retain the nanofiber architecture after immersed in water, which prohibits their usage in aqueous medium for the application of metal-ion sensing. Thus, the introduction of NMA moieties provides the thermally crosslinking functionality for maintaining the nanofibrous morphology. Figure 2 shows the FE-SEM images of PNNR2 nanofibers in various states, and the insert SEM image in Fig. 2a shows a smooth and nonporous surface of PNNR2 nanofibers, similar to those reported in previous studies [15]. After thermal curing at 110 °C for 72 h, nanofibers remained the original structure [Fig. 2b] with similar diameters (277 ± 58 and 270 ± 28 nm for PNNR2 and PNNR3 crosslinked nanofibers, respectively). To explore the influence of water immersion on the morphologies of the ES nanofibers, the crosslinked nanofibers immersed in water for 30 min were processed carefully with liquid nitrogen to retain the morphologies. As shown in Fig. 2c, PNNR2 ES nanofibers were not soluble in water and

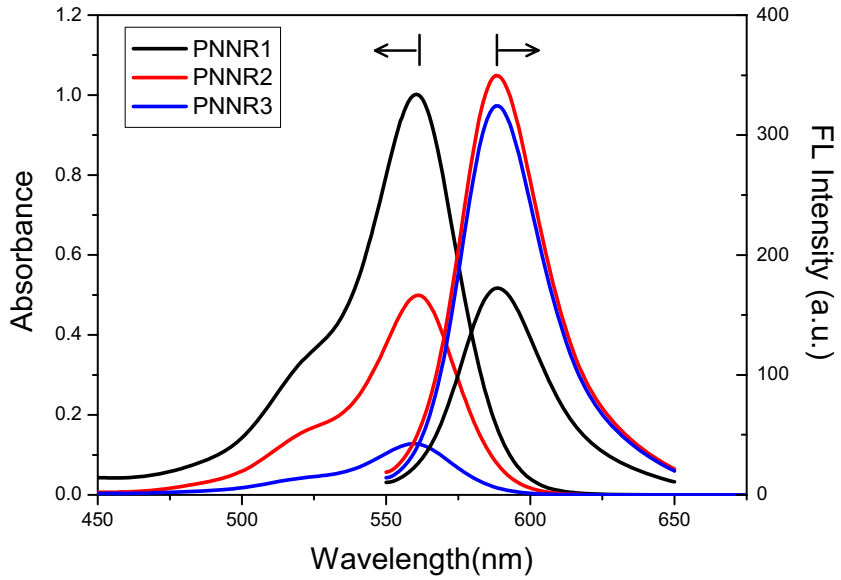

Fig. 3 Absorption and photoluminescence spectra of PNNR in methanol/Tris–HCl buffer (*v*/*v* = 2) at pH 3.6

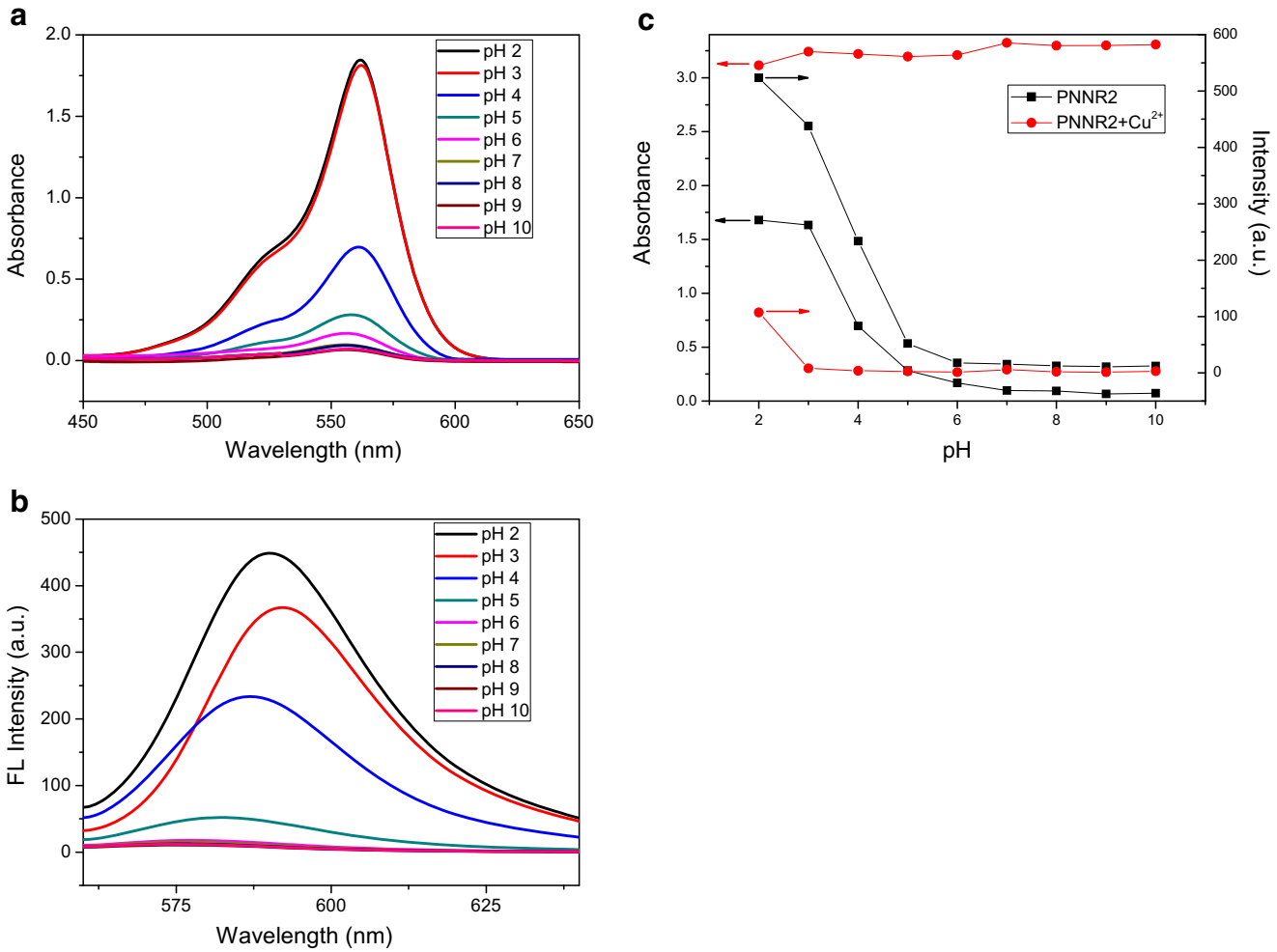

Fig. 4 Absorption (**a**) and photoluminescence (**b**) spectra of PNNR2 in methanol/Tris–HCl buffer ($v/v = 2$) at a RB concentration of 10^{-4} M at various pH values. (**c**) Absorbance and fluorescence intensity of PNNR2 in methanol/Tris–HCl buffer ($v/v = 2$) at a RB concentration of 10^{-4} M as functions of pH with or without addition of Cu^{2+} (10^{-4} M)

maintained their fiber morphologies, attributed to the thermal cross-linking of the NMA moiety [34]. The average diameters of the PNNR2 and PNNR3 ES nanofibers after immersion in water are expanded to 1046 ± 215 and 1179 ± 291 nm, respectively, resulting from the swelling of nanofibers due to the hydrophilic NIPAAm moieties. This electrospun mat with nonwoven nanofibrous structure provides a surface area-to-volume ratio about 1–2 orders of magnitude higher than that of continuous thin film [35], which guarantees a much higher contact area in the solid–liquid interface. For comparison, the continuous thin films of PNNR copolymers were also prepared via dip-coating method. Both the ES film and dip-coating film were thermally cured at 110 °C for 72 h before optical measurement.

Fluorescent response of PNNR copolymers to proton and Cu^{2+} ions

The rhodamine fluorochrome could act as a fluorophore and chromophore probe based on the spirolactam ring-opening process [28]. Recently, Yang et al. reported a rhodamine-based sensor for selectively detection of Cu^{2+} and Hg^{2+} ions [23]. In particular, this sensor showed high absorbance but low fluorescence after Cu^{2+} recognition due to the fluorescence quenching of paramagnetic effect of the d_9 system of Cu^{2+} ion [36]. Herein, to build up an "ON-OFF" type of fluorescent sensor for Cu^{2+} ions (Scheme S1), we first activated RHPMA moieties on prepared copolymers in the acidic environment to display a pink color and strong fluorescence, and then monitored the fluorescence quenching due to Cu^{2+} ion detection. Figure 3 represents the absorption and photoluminescence spectra of PNNR copolymers in methanol/Tris–HCl buffer ($v/v = 2$) at pH 3.6. The values of maximum absorbance around 556 nm showed increment with higher RHPMA content, but the fluorescence intensity showed dramatic decrease for PNNR1 with the highest RHPMA content which might be resulted from the aggregation-caused quenching. Figure 4 shows the absorption and photoluminescence spectra of PNNR2 in methanol/Tris–HCl buffer ($v/v = 2$) at a RB concentration of 10^{-4} M at various

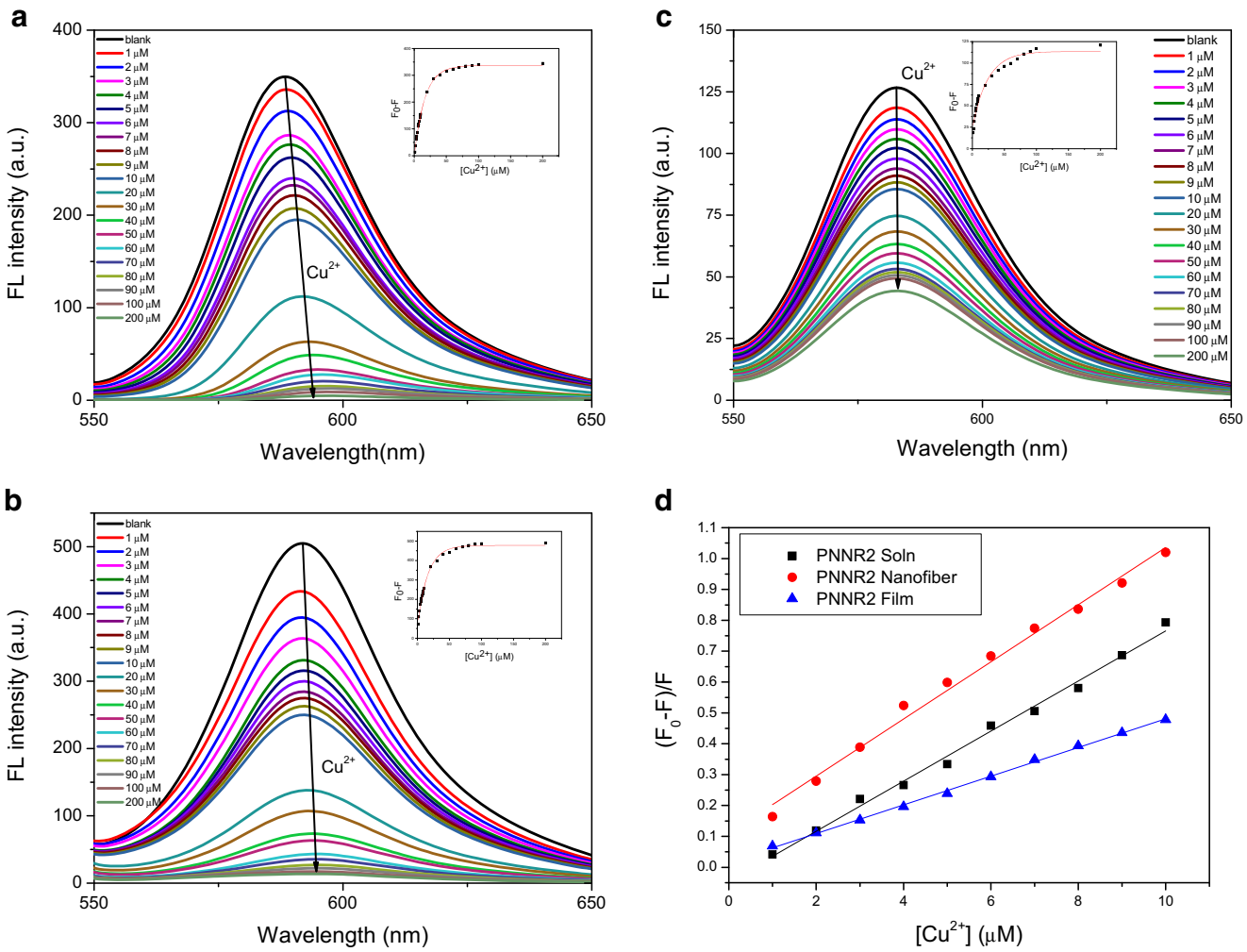

Fig. 5 Fluorescence spectra of PNNR2 solution in methanol/Tris–HCl buffer (*v*/*v* = 2) at a RB concentration of 10^{-4} M at pH 3.6 (**a**), PNNR2 nanofibers (**b**) and PNNR2 dip-coated films (**c**) in methanol/Tris–HCl buffer (*v*/*v* = 2) at pH 3.6 upon the addition of different concentrations of Cu^{2+} ions. The insets represent fluorescence quenching as a function of Cu^{2+} concentration. (**d**) Stern-Volmer plots of PNNR2 in different states for Cu^{2+} detection

pH values. At pH values larger than 6, PNNR2 solution showed very weak absorption and emission. After protonation and formation of open-ring amide structure in RHPMA moieties at pH value smaller than 6, absorbance and emission intensity of PNNR2 solution showed increment with increasing acidity. As shown in Fig. 4c, the variations of absorbance and emission intensity of PNNR2 solution with or without addition of Cu^{2+} ions (10^{-4} M) are plotted as functions of pH value. With addition of Cu^{2+} ions, formation of open-ring amide structure resulted in strong absorption even at pH value larger than 6. However, emission was quenched due to the paramagnetic effect of the d_9 system of Cu^{2+} ion [36]. The abnormal behavior of fluorescence enhancement at pH = 2 might be attributed to the competition between protonation and metal chelation at this strong acidic condition. Thus, in the following investigation, the sensing performance of PNNR copolymers in different states were carried out in a fixed pH value of 3.6 to make sure clear fluorescence quenching upon Cu^{2+} binding. The stoichiometry of Cu^{2+} coordination with RHPMA moieties was investigated by the Job's plot (Fig. S4), which indicated that a 1:1 coordination between Cu^{2+} and the RHPMA moiety was the most possible binding mode.

Fluorescence titration for PNNR copolymers upon Cu^{2+} binding in different states

The performance of P(NIPAAm-*co*-NMA-*co*-RhBMA) copolymers for copper ion sensing was explored in different states, including solution, thin film and nanofiber, by fluorescence titration of Cu^{2+} ions. Figure 5a shows the variation in the fluorescence spectra of PNNR2 solution in the presence of Cu^{2+} ions at different concentration (corresponding titration spectra for PNNR1 and PNNR3 are shown in Fig. S5). Upon titrating with Cu^{2+} ions, a gradual quenching of fluorescence was observed with the increase of Cu^{2+} concentration. The

Table 2 Stern-Volmer constants (K_{sv}) for PNNR copolymers in different states

Polymer	Soln. [10^4 M^{-1}]	Nanofiber [10^4 M^{-1}]	Film [10^4 M^{-1}]
PNNR1	9.28	N/A	2.87
PNNR2	8.11	9.25	4.65
PNNR3	8.01	13.0	6.03

plots of fluorescence quenching as a function of Cu^{2+} concentration showed the ES nanofibers had high sensitivity at the response concentration range of 1×10^{-6} to 1×10^{-5} M (inset of Fig. 5a). Similar variation of fluorescence quenching was observed for the copper ion titration of PNNR nanofibers (Fig. 5b for PNNR2 nanofibers and Fig. S6 for PNNR3 nanofibers). However, for dip-coating PNNR films (Fig. 5c for PNNR2 film and Fig. S7 for PNNR1 and PNNR3 films, respectively), the fluorescent quenching became less sensitive toward Cu^{2+} concentration, indicating poorer accessibility of rhodamine moieties to the quencher (Cu^{2+} ions) in polymer thin films. The quantitative evaluation of the fluorescent quenching phenomenon can be accomplished by the Stern-Volmer plot (Fig. 5d). Linear relationship for Cu^{2+} ions was observed in the concentration range of 1–10 μM, and the Stern-Volmer constants (K_{sv}) estimated from the slopes are 9.28×10^4, 8.11×10^4, and 8.01×10^4 M^{-1} for PNNR1, PNNR2 and PNNR3 in solution, respectively. The higher K_{sv} value of PNNR1 solution for Cu^{2+} ions relative to PNNR2 and PNNR3 solutions indicated the more sensitive of PNNR1 in solution state due to the highest RHPMA content. The Stern-Volmer constants (K_{sv}) for PNNR2 and PNNR3 nanofibers are 9.25×10^4 and 1.30×10^5 M^{-1}, respectively. The lower K_{sv} value of PNNR2 nanofibers might be due to potential aggregation of rhodamine moieties in nanofibers which hindered the Cu^{2+} binding. Among three different states, copolymer thin films showed lowest K_{sv} values as compared to solutions and nanofibers (Table 2). This might be due to diffusional retardation of metal ions in the solid state in addition with much lower surface area-to-volume ratio of thin films.

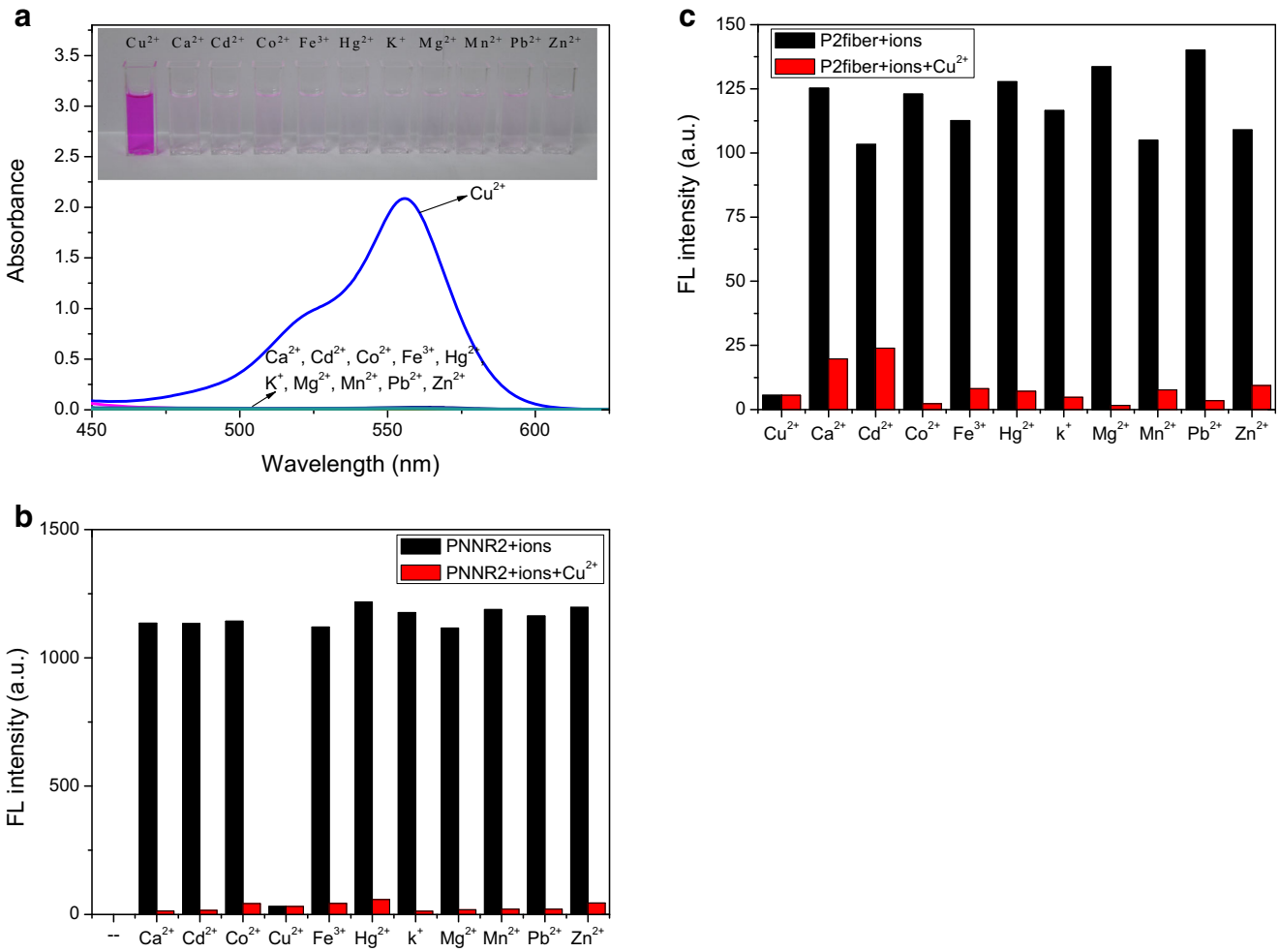

Fig. 6 (**a**) Absorption spectra of PNNR2 in methanol/Tris–HCl buffer ($v/v = 2$) at a RB concentration of 10^{-4} M at pH 7 upon the addition of various metal ions (10^{-4} M). The insets in (**a**) represent photographs PNNR2 solutions with addition of various metal ions. Competition tests of PNNR2 solutions (**b**) and nanofibers (**c**) against representative metal ions

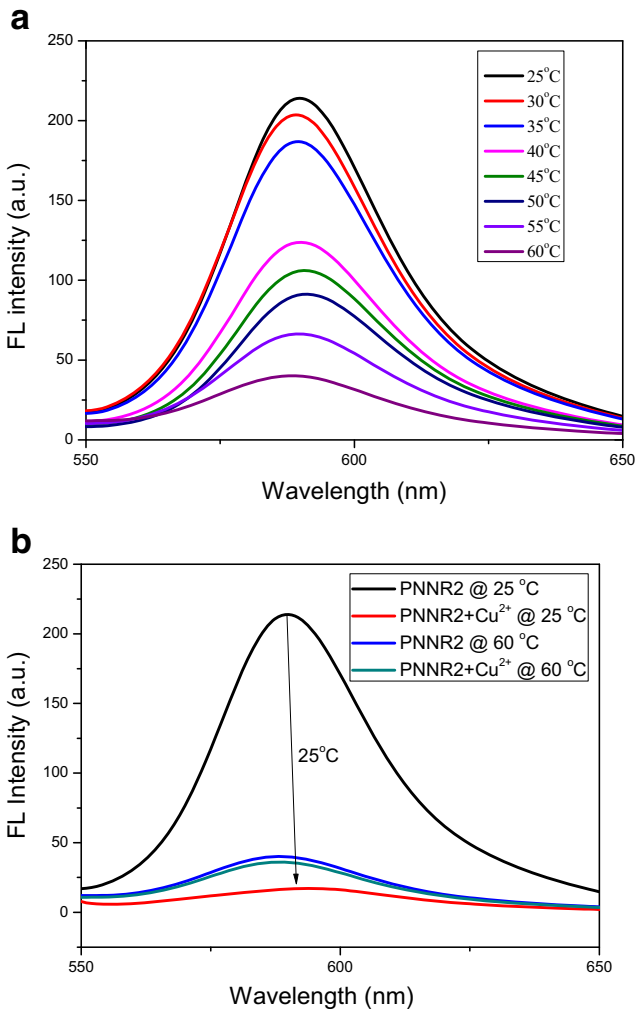

Fig. 7 (**a**) Fluorescence spectra of PNNR2 nanofibers in methanol/Tris–HCl buffer (*v/v* = 2) at pH 3.6 in the temperature range of 25–60 °C. (**b**) Fluorescence spectra of PNNR2 nanofibers before and after addition of Cu^{2+} (10^{-4} M) at 25 and 50 °C, respectively

Selectivity and tolerance of PNNR toward Cu^{2+}

Figure 6a shows the absorption spectra of PNNR2 in methanol/Tris–HCl buffer (*v/v* = 2, pH = 7) at a RB concentration of 10^{-4} M with addition of various metal ions (10^{-4} M). Strong absorption with maximum at 556 nm and pink color was observed only with addition of Cu^{2+} ions (inset images). To further evaluate the "ON/OFF" fluorescence detection of PNNR copolymers upon Cu^{2+} binding, competition studies were carried out in the presence of other representative metal ions, including Ca^{2+}, Cd^{2+}, Co^{2+}, Fe^{3+}, Hg^{2+}, K^{+}, Mg^{2+}, Mn^{2+}, Pb^{2+}, and Zn^{2+}. Significant fluorescence quenching was observed only after addition of Cu^{2+}, regardless of competing ions, in both states of solution (Fig. 6b) and nanofiber (Fig. 6c). This observation further elucidates that PNNR copolymers has a superior selectivity toward Cu^{2+} than other competitive metal ions.

Thermo-responsive "ON-OFF" sensitivity and chemical reversibility test of PNNR nanofibers

Figure 7a shows the effect of temperature on the fluorescence spectra of PNNR2 nanofibers. The fluorescence of PNNR2 nanofibers decreased with increasing temperature from 25 to 60 °C. The thermo-responsive fluorescent characteristics can be correlated with the swollen-shrunk transition of nanofibers with varying temperature in aqueous medium. When temperature increases around the LCST, the intermolecular hydrogen bonding between amide moiety of PNIPAAm and water molecules becomes weak and undergoes hydrophilic-hydrophobic transition, which leads to the deswelling of nanofibers to squeeze out of the water molecules. The shrink causes rhodamine moieties more compact in the nanofibers and results in the suppression of fluorescence due to aggregation-caused quenching. To evaluate the thermo-responsive sensing characteristics of PNNR nanofibers, the fluorescence spectra of PNNR2 nanofibers were monitored at 25 and 60 °C, respectively, before and after Cu^{2+} binding. As shown in Fig. 7b, the fluorescent quenching was observed at 25 °C upon Cu^{2+} addition due to high accessibility of ions for the nanofibers swelling with water, suggesting the nanofibers exhibiting "ON" state for Cu^{2+} sensing. In contrast, only slight fluorescence quenching at 60 °C indicated the "OFF" state toward Cu^{2+} ions, resulting from the hydrophilic-hydrophobic transition around LCST that impeded the Cu^{2+} ions from complexation with RHPMA moieties. These results indicate the PNNR nanofibers have the potential as a thermo-responsive on-off senor for Cu^{2+} detection.

The reversibility and stability of prepared PNNR nanofibers were investigated by EDTA-regeneration experiments. As shown in Fig. 8, the fluorescence of PNNR2 nanofibers showed fully reversible quenching/recovery cycles upon alternating treatment with Cu^{2+} and EDTA. This successfully regeneration by EDTA suggests that PNNR nanofibers could be reused with proper treatment. In addition with the easy separation from aqueous solution, PNNR nanofibers would be a potential material system for highly sensitive and economical sensor devices.

Conclusions

In summary, a series of random copolymers, poly(*N*-isopropylacrylamide)-*co*-poly(*N*-methylolacrylamide)-*co*-poly(RHPMA) [Poly(NIPAAm-*co*-NMA-*co*-RHPMA), PNNR], was synthesized via a free radical polymerization, and the corresponding nanofibrous mats were prepared via electrospinning technique for detection of copper (Cu^{2+}) ions. The PNNR copolymers exhibited superior selectivity and sensitivity and demonstrated "ON-OFF" fluorescence change upon Cu^{2+} binding. By comparing the Stern-Volmer constants of

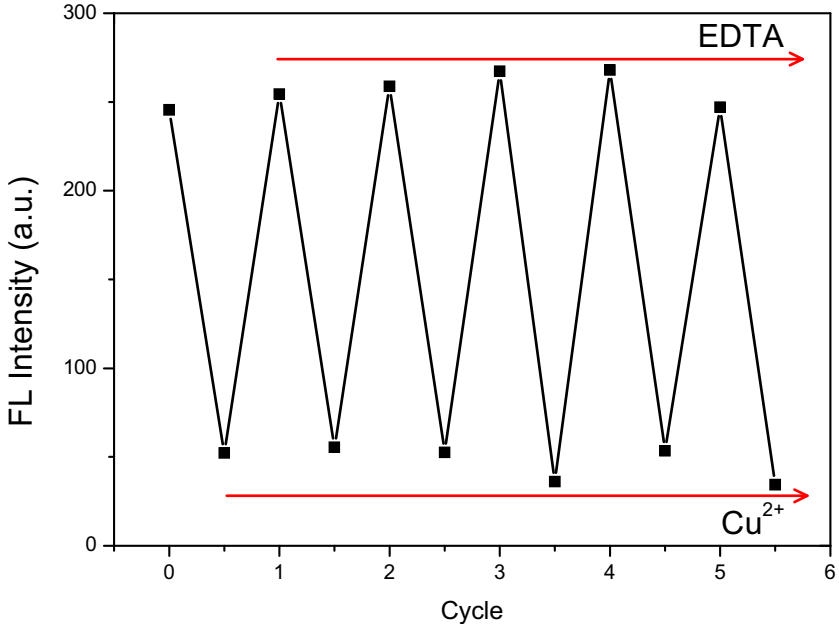

Fig. 8 Fluorescence responses of PNNR2 nanofibers by alternating treatment of Cu^{2+} and Na_4EDTA

PNNR copolymers in solutions, nanofibers and dip-coated films, PNNR nanofibers displayed much higher sensitivity as compared to films and showed similar characteristics as solutions due to the higher surface/volume ratio of nanofibrous structure. The PNNR nanofibers also showed an interesting thermo-responsive on-off switching sensitivity in response to the hydrophilic-hydrophobic transition of PNIPAAm segments. Furthermore, the fluorescence response of PNNR toward Cu^{2+} is chemically reversible both in solution and in nanofibers. Further effort will focus on roll-to-roll preparation of PNNR nanofibers and exploring the potential applications in pollutant separation and water purification.

Acknowledgments The financial support from the Ministry of Science and Technology of Taiwan is highly appreciated. This research was also supported in part by the Headquarters of University Advancement at the National Cheng Kung University, which is sponsored by the Ministry of Education, Taiwan, ROC.

Supporting information on ^{1}H-NMR spectra of RHPMA, LCST test of PNNR copolymers, Job's plot, and titration data for thin films is available online.

References

1. Lorber KE (1986) Monitoring of heavy metals by energy dispersive X- ray fluorescence spectrometry. Waste Manag Res 4(1):3–13
2. Bings NH, Bogaerts A, Broekaert JAC (2006) Atomic spectroscopy. Anal Chem 78(12):3917–3946
3. Nolan EM, Lippard SJ (2008) Tools and tactics for the optical detection of mercuric ion. Chem Rev 108(9):3443–3480
4. Zhang J, Yuan Y, Wang Y, Sun F, Liang G, Jiang Z, Yu S-H (2015) Microwave-assisted synthesis of photoluminescent glutathione-capped Au/Ag nanoclusters: a unique sensor-on-a-nanoparticle for metal ions, anions, and small molecules. Nano Res 8(7):2329–2339
5. Liu B, Yu W-L, Pei J, Liu S-Y, Lai Y-H, Huang W (2001) Design and synthesis of bipyridyl-containing conjugated polymers: effects of polymer rigidity on metal ion sensing. Macromolecules 34(23): 7932–7940
6. Hong W, Li W, Hu X, Zhao B, Zhang F, Zhang D (2011) Highly sensitive colorimetric sensing for heavy metal ions by strong polyelectrolyte photonic hydrogels. J Mater Chem 21(43):17193
7. Çeken B, Kandaz M, Koca A (2012) Electrochemical metal-ion sensors based on a novel manganese phthalocyanine complex. Synth Met 162(17–18):1524–1530
8. Valeur B (2002) Molecular fluorescence: principle and application. Wiley-VCH, Weinheim
9. Carter KP, Young AM, Palmer AE (2014) Fluorescent sensors for measuring metal ions in living systems. Chem Rev 114(8): 4564–4601
10. III SWT, Joly GD, Swager TM (2007) Chemical sensors based on amplifying fluorescent conjugated polymers. Chem Rev 107(4): 1339–1386
11. You J, Kim J, Park T, Kim B, Kim E (2012) Highly fluorescent conjugated polyelectrolyte nanostructures: synthesis, self-assembly, and Al3+ ion sensing. Adv Funct Mater 22(7):1417–1424
12. Jaiswal A, Ghsoh SS, Chattopadhyay A (2012) Quantum dot impregnated-chitosan film for heavy metal ion sensing and removal. Langmuir 28(44):15687–15696
13. Lou Y, Zhao Y, Chen J, Zhu J-J (2014) Metal ions optical sensing by semiconductor quantum dots. J Mater Chem C 2(4):595–613
14. Lv F, Feng X, Tang H, Liu L, Yang Q, Wang S (2011) Development of film sensors based on conjugated polymers for copper (II) ion detection. Adv Funct Mater 21(5):845–850
15. Chen L-N, Weng N-K, Wu W-C, Chen W-C (2015) Electrospun polymer nanofibers of P(NIPAAm-co-SA-co-FBPY): preparation, structural control, metal ion sensing and thermoresponsive characteristics. Mater Chem Phys 163:63–72
16. Uauy R, Olivares M, Gonzalez M (1998) Essentiality of copper in humans. Am J Clin Nutr 67(5):952S–959S
17. Brown DR, Kozlowski H (2004) Biological inorganic and bioinorganic chemistry of neurodegeneration based on prion and Alzheimer diseases. Dalton Trans 13:1907–1917
18. Barnham KJ, Masters CL, Bush AI (2004) Neurodegenerative diseases and oxidative stress. Nat Rev Drug Discov 3(3):205–214

19. Bull PC, Thomas GR, Rommens JM, Forbes JR, Cox DW (1993) The Wilson disease gene is a putative copper transporting P-type ATPase similar to the Menkes gene. Nat Genet 5(4): 327–337
20. Sivaraman G, Anand T, Chellappa D (2013) Quick accessible dual mode turn-on red fluorescent chemosensor for Cu(ii) and its applicability in live cell imaging. RSC Adv 3(38):17029
21. Yang Y, Zhao Q, Feng W, Li F (2013) Luminescent chemodosimeters for bioimaging. Chem Rev 113(1):192–270
22. Wang M, Yan F, Zou Y, Chen L, Yang N, Zhou X (2014) Recognition of Cu2+ and Hg2+ in physiological conditions by a new rhodamine based dual channel fluorescent probe. Sensors Actuators B Chem 192:512–521
23. Yang Y, Gao C, Li B, Xu L, Duan L (2014) A rhodamine-based colorimetric and reversible fluorescent chemosensor for selectively detection of Cu2+ and Hg2+ ions. Sensors Actuators B Chem 199: 121–126
24. Zhang JF, Zhou Y, Yoon J, Kim Y, Kim SJ, Kim JS (2010) Naphthalimide modified rhodamine derivative: ratiometric and selective fluorescent sensor for Cu2+ based on two different approaches. Org Lett 12(17):3852–3855
25. Zhou Z, Li N, Tong A (2011) A new coumarin-based fluorescence turn-on chemodosimeter for Cu2+ in water. Anal Chim Acta 702(1):81–86
26. Wang D, Shiraishi Y, Hirai T (2011) A BODIPY-based fluorescent chemodosimeter for Cu(II) driven by an oxidative dehydrogenation mechanism. Chem Commun 47(9):2673–2675
27. Basu A, Das G (2011) Oxidative cyclization of thiosemicarbazone: an optical and turn-on fluorescent chemodosimeter for Cu(II). Dalton Trans 40(12):2837–2843
28. Kim HN, Lee MH, Kim HJ, Kim JS, Yoon J (2008) A new trend in rhodamine-based chemosensors: application of spirolactam ring-opening to sensing ions. Chem Soc Rev 37(8):1465–1472
29. Xiang Y, Tong A, Jin P, Ju Y (2006) New fluorescent rhodamine hydrazone chemosensor for Cu(II) with high selectivity and sensitivity. Org Lett 8(13):2863–2866
30. Xu Z, Zhang L, Guo R, Xiang T, Wu C, Zheng Z, Yang F (2011) A highly sensitive and selective colorimetric and off–on fluorescent chemosensor for Cu2+ based on rhodamine B derivative. Sensors Actuators B Chem 156(2):546–552
31. Feil H, Bae YH, Feijen J, Kim SW (1993) Effect of comonomer hydrophilicity and ionization on the lower critical solution temperature of N-isopropylacrylamide copolymers. Macromolecules 26(10):2496–2500
32. Sun G, Zhang XZ, Chu CC (2007) Formulation and characterization of chitosan-based hydrogel films having both temperature and pH sensitivity. J Mater Sci Mater Med 18(8):1563–1577
33. Na H, Liu X, Li J, Zhao Y, Zhao C, Yuan X (2009) Formation of core/shell ultrafine fibers of PVDF/PC by electrospinning via introduction of PMMA or BTEAC. Polymer 50(26):6340–6349
34. Chen L-N, Chiu Y-C, Hung J-J, Kuo C-C, Chen W-C (2014) Multifunctional electrospun nanofibers prepared from poly((N-isopropylacrylamide)-co-(N-hydroxymethylacrylamide)) and their blends with 1,2-diaminoanthraquinone for NO Gas detection. Macromol Chem Phys 215(3):286–294
35. Wang X, Drew C, Lee S-H, Senecal KJ, Kumar J, Samuelson LA (2002) Electrospun nanofibrous membranes for highly sensitive optical sensors. Nano Lett 2(11):1273–1275
36. Kim JS, Quang DT (2007) Calixarene-derived fluorescent probes. Chem Rev 107(9):3780–3799